Sensors and Materials, Vol. 37, No. 2 (2025) 519–524
MYU Tokyo

S & M 3927

Radio- and Photoluminescence Properties of Nd-doped Barium Chloride Transparent Ceramic and Single Crystal

Shota Otake,* Shunta Takase, Takumi Kato,
Daisuke Nakauchi, Noriaki Kawaguchi, and Takayuki Yanagida

Nara Institute of Science and Technology (NAIST), 8916-5 Takayama-cho, Ikoma-shi, Nara 630-0192, Japan

(Received September 10, 2024; accepted December 12, 2024)

Keywords: near-infrared luminescence, scintillation, ionizing radiation, transparent ceramics, single crystals

1.0% Nd-doped $BaCl_2$ transparent ceramic and single crystal samples were respectively prepared by spark plasma sintering and the vertical Bridgman–Stockbarger method to compare their optical and scintillation properties. The photoluminescence quantum yield of the crystal sample was 5.4% under 580 nm excitation, whereas that of the ceramic sample was below the detection limit of the device. In the scintillation spectra, multiple emission peaks derived from 4f–4f transitions of Nd^{3+} were observed in the 530–1330 nm range for both samples. For the dose rate response function, the lower detection limits of the ceramic and crystal samples were 0.03 and 0.003 Gy/h, respectively. Our samples had better detection limits than previously reported values of Nd:CsI (0.06 Gy/h) and Nd:$CaWO_4$ (0.06 Gy/h) single crystals.

1. Introduction

Scintillators are phosphor materials that immediately convert ionizing radiation into low-energy photons.[1–3] They are widely used for radiation detection in combination with photodetectors.[4,5] Since conventional photodetectors have wavelength sensitivity in the ultraviolet–visible (UV–Vis) range, scintillators that emit photons at 300–600 nm, such as Ce:$LaBr_3$, Eu:SrI_2, Tl:NaI, Ce:$Y_3Al_5O_{12}$ (YAG), and Ce:$Gd_3(Al, Ga)_5O_{12}$, have been used so far.[6] In addition, scintillators are typically required to have high light yield, high effective atomic number (Z_{eff}), and chemical stability.[7,8]

Recently, some new photodetectors with high wavelength sensitivity in the near-infrared (NIR) region from 800 to 2000 nm have been developed,[9,10] and scintillators with emission peaks in the NIR region (NIR scintillators) have attracted much attention.[11] NIR scintillators are expected to be applied to radiation detection in high-dose fields because of the following two advantages. First, their emission can easily be distinguished from Cherenkov light, which appears in the UV–Vis range in high-dose fields. When conventional scintillators are used, the Cherenkov light overlaps with the scintillation signal, leading to incorrect radiation measurements; therefore, the use of NIR scintillators is expected to reduce noise.[12] Second,

*Corresponding author: e-mail: otake.shota.os4@ms.naist.jp
https://doi.org/10.18494/SAM5433

ISSN 0914-4935

NIR photons can propagate through optical fibers with high efficiency. In high-dose fields, the use of long-distance optical fibers (tens to hundreds of meters) for remote monitoring has been proposed.[13,14] Commonly used quartz fibers have a higher propagation efficiency in the NIR region than in the visible one, and radiation detectors using NIR scintillators can read scintillation light with less loss.[15,16] For the above reasons, the development of NIR scintillators is significant.

In this study, we propose Nd:$BaCl_2$ as a new NIR scintillator. $BaCl_2$ (Z_{eff} = 51) has a high Z_{eff} comparable to those of commercially used NaI (Z_{eff} = 51), SrI_2 (Z_{eff} = 50), and $LaBr_3$ (Z_{eff} = 47) scintillators. While the above commercial scintillators have hygroscopicity, $BaCl_2$ has low hygroscopicity and can be easily used under atmosphere. $BaCl_2$ doped with Eu has been investigated in detail for scintillation properties,[17–19] and its *LY* was equivalent to that of commercial Tl:NaI scintillators.[17,20] On the other hand, Nd^{3+} shows highly efficient luminescence in the NIR range and has been actively studied as a luminescent center for NIR scintillators in recent years.[21,22] Therefore, Nd:$BaCl_2$ is also expected to exhibit excellent scintillation properties in the NIR region. To demonstrate its scintillation performance, Nd:$BaCl_2$ was fabricated in transparent ceramic (TC) and single crystal (SC) material forms.

2. Experimental Methods

Nd:$BaCl_2$ TC and SC samples were respectively prepared by spark plasma sintering (SPS) and the vertical Bridgman–Stockbarger method. Raw powders of $NdCl_3$ $6H_2O$ (>99.9%, Nippon Yttrium) and $BaCl_2$ (>99.99%, Rare Metals) were uniformly mixed at a molar ratio of 1:99 using a mortar and pestle. The mixture was then dried at 400 °C for 3 h with a small electric furnace under vacuum to remove water. In the fabrication of the Nd:$BaCl_2$ TC sample, the dried mixture was sealed in a graphite die and two punches and sintered using SPS equipment (LABOX-300, Sinterland). The details of the sintering conditions were based on our past report.[18,23] For the SC sample preparation, the dried mixture was sealed with a gas burner (KSA-22, Tokyo Koshin) and then loaded into a Bridgman furnace (VFK-1800, Crystal Systems). The heating temperature in the furnace was set at 1000 °C, and the pull-down rate was 3 mm/h.

Diffuse transmittance spectra were evaluated using a spectrophotometer (Shimadzu, SolidSpec-3700) over the spectral range of 200–1650 nm. Photoluminescence (PL) emission and excitation maps and quantum yields (QYs) were measured using Quantaurus-QY (C11347, Hamamatsu Photonics). PL decay profiles were evaluated using Quantaurus-τ (C11367, Hamamatsu Photonics). To measure the scintillation characteristics, X-ray-induced scintillation spectra,[24] afterglow profiles,[25] and dose rate response functions[26] were determined using our original equipment. Detailed information and conditions can be found in the references.

3. Results and Discussion

Figure 1 shows the diffuse transmittance spectra, while the inset shows the photographs of the prepared Nd:$BaCl_2$ TC and SC samples. The TC and SC samples were unified to a thickness of approximately 0.9 mm, and their masses were 0.122 and 0.038 g, respectively. The transmittances of the TC and SC samples in the spectral range longer than 850 nm were

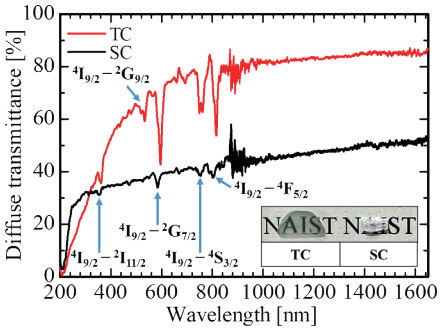

Fig. 1. (Color online) Diffuse transmittance spectra. The inset shows photographs of the prepared samples.

approximately 80 and 50%, respectively. $BaCl_2$ has a phase transition between cubic and orthorhombic phases near 920 °C,[27] so the SC sample contained some cracks and showed a lower transmittance than the TC sample. Absorption peaks observed at 355, 535, 595, 760, and 820 nm would be due to $^4I_{9/2}$–$^2I_{11/2}$, $^2G_{9/2}$, $^2G_{7/2}$, $^4S_{3/2}$, and $^4F_{5/2}$ transitions of Nd^{3+}, respectively.[28] The spectra in the range of 850–1000 nm were affected by noise due to detector switching. In addition, the hygroscopicity of $BaCl_2$ (>99.99%, Rare Metals) and NaI (>99.999%, Sigma Aldrich) powders in air was evaluated by comparing the mass increasing rate (temperature: 19.7 °C; humidity: 57.2%). Those of the $BaCl_2$ and NaI powders after 2 h were respectively 1.5 and 3.5%, indicating that $BaCl_2$ had a lower hygroscopicity than NaI.

Figure 2 depicts the PL emission and excitation maps when irradiated with excitation light from 250 to 850 nm every 10 nm interval. PL intensities of the TC sample were too weak to detect emission peaks, while the SC sample showed clear emission peaks at 890 and 1060 nm, which were derived from the $^4F_{3/2}$–$^4I_{9/2}$ and $^4F_{3/2}$–$^4I_{11/2}$ transitions of Nd^{3+}, respectively.[29] The PL *QY* of the SC sample was 5.4% under 580 nm excitation, and that of the TC sample was below the detection limit of the device. These values are lower than those of other Nd-doped scintillators.[28,30]

The PL decay curves monitored at 890 nm under 575–625 nm excitation are exhibited in Fig. 3. Both decay curves were consistent with an approximation using a single exponential decay function, and the samples showed similar decay time constants of approximately 210 μs. These decay time constants were reasonable for the $^4F_{3/2}$–$^4I_{9/2}$ transition of Nd^{3+}.[28,31]

Figure 4 shows the X-ray-induced scintillation spectra in the 200–1600 nm range. In the spectra at 250–500 nm, emission peaks at 310 and 410 nm might be due to self-trapped excitons and defects or impurities, respectively.[32] These peaks overlapped with the Nd^{3+} absorption wavelengths at 305, 330, 345, and 355 nm.[29] All the sharp emission peaks at 530–1330 nm were consistent with Nd^{3+} luminescence in previous reports.[29,33]

Figure 5 shows the afterglow profiles. Afterglow levels were calculated using the equation shown in the figure. The afterglow levels of the TC and SC samples were respectively estimated to be 1160 and 890 ppm. These values correspond to the number of trapping centers with a shallow energy level, suggesting that the SC sample is more efficient than the TC sample in the energy transfer process. In addition, the afterglow levels of the Nd:$BaCl_2$ samples are inferior to those of other 1.0% Nd-doped scintillators,[28,30,31] so the afterglow values of the samples need to be improved.

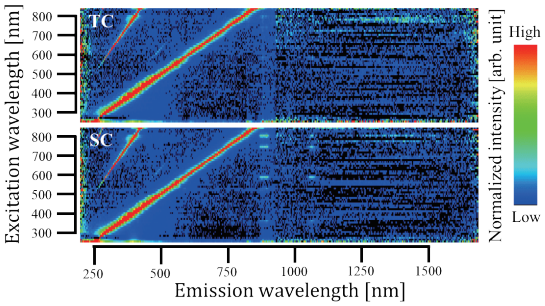

Fig. 2. (Color online) PL emission and excitation maps of the TC (top) and SC samples (bottom).

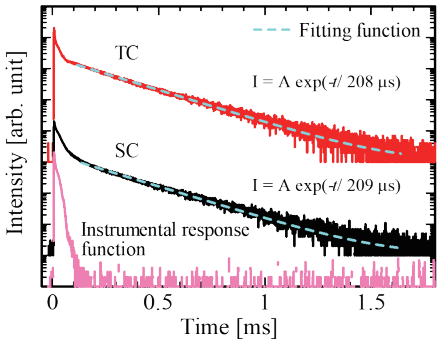

Fig. 3. (Color online) PL decay curves.

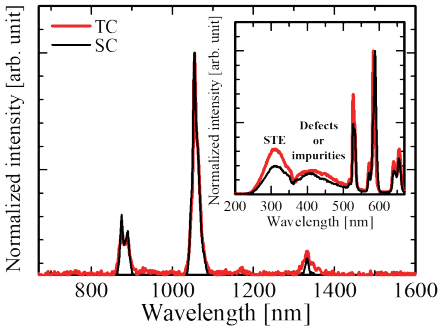

Fig. 4. (Color online) X-ray-induced scintillation spectra. The inset shows the spectra in the 200–670 nm range.

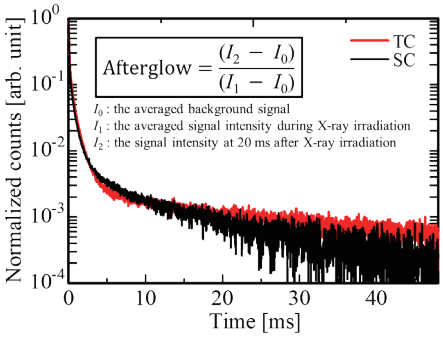

Fig. 5. (Color online) Afterglow profiles.

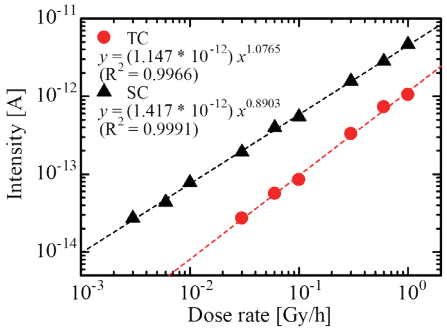

Fig. 6. (Color online) Dose rate response functions in the NIR region.

The dose rate response functions in the NIR region are exhibited in Fig. 6. The vertical axis represents the average intensity during X-ray irradiation subtracted by the average background intensity, and the horizontal axis indicates the dose rate. The calculated values on the vertical axis were corrected for the mass ratio of the samples. The lower detection limits with linearity for the TC and SC samples were 0.03 and 0.003 Gy/h, respectively. On the basis of Robbins' theoretical formula,[34] it is possible that PL *QY* and afterglow contributed to the difference in the dose rate response of the samples. On the other hand, the fact that both samples showed better detection limits than the Nd:CsI (0.06 Gy/h)[31] and Nd:$CaWO_4$ (0.06 Gy/h)[30] SCs indicates that Nd:$BaCl_2$ has high potential as an NIR scintillator.

4. Conclusions

We have fabricated 1.0% Nd-doped $BaCl_2$ TC and SC samples and characterized their properties. Regarding their optical properties, the diffuse transmittances of the TC and SC samples in the NIR region were approximately 80 and 50%, respectively, and the absorption due to Nd^{3+} was observed in the range of 350–850 nm. The PL *QY* of the SC sample was 5.4% under 580 nm excitation, whereas that of the TC sample was below the detection limit of the device. In the scintillation spectra, multiple emission peaks derived from Nd^{3+} were observed in the 530–1330 nm range for both samples. The lower detection limits for the TC and SC samples under X-ray irradiation were 0.03 and 0.003 Gy/h, respectively. The obtained results showed that the Nd:$BaCl_2$ SC had better properties than the TC sample as an NIR scintillator.

Acknowledgments

This work was supported by MEXT Grants-in-Aid for Scientific Research A (22H00309), Scientific Research B (23K21827,23K25126 and 24K03197), Exploratory Research (22K18997), and Early-Career Scientists (23K13689).

References

1 K. Watanabe: Jpn. J. Appl. Phys. **62** (2023) 010507. https://doi.org/10.35848/1347-4065/ac90a5
2 M. Koshimizu: Jpn. J. Appl. Phys. **62** (2023) 010503. https://doi.org/10.35848/1347-4065/ac94fe
3 T. Kato, D. Nakauchi, N. Kawaguchi, and T. Yanagida: Sens. Mater. **36** (2024) 531. https://doi.org/10.18494/SAM4749
4 T. Yanagida, T. Kato, D. Nakauchi, and N. Kawaguchi: Jpn. J. Appl. Phys. **62** (2023) 010508. https://doi.org/10.35848/1347-4065/ac9026
5 T. Yanagida: Proc. Jpn. Acad. Ser. B **94** (2018) 75. https://doi.org/10.2183/pjab.94.007
6 H. Kimura, H. Fukushima, K. Watanabe, T. Fujiwara, H. Kato, M. Tanaka, T. Kato, D. Nakauchi, N. Kawaguchi and T. Yanagida: Sens. Mater. **36** (2024) 507. https://doi.org/10.18494/SAM4767
7 T. Yanagida, K. Watanabe, T. Kato, D. Nakauchi, and N. Kawaguchi: Sens. Mater. **35** (2023) 423. https://doi.org/10.18494/SAM4135
8 P. Kantuptim, T. Kato, D. Nakauchi, N. Kawaguchi, K. Watanabe, and T. Yanagida: Sens. Mater. **35** (2023) 451. https://doi.org/10.18494/SAM4141
9 S. Simingalam, B. L. VanMil, Y. Chen, E. A. DeCuir, G. P. Meissner, P. Wijewarnasuriya, N. K. Dhar, and M. V. Rao: Solid State Electron. **101** (2014) 90. https://doi.org/10.1016/j.sse.2014.06.037
10 M. Vollmer, K.-P. Möllmann, and J. A. Shaw: Education and Training in Optics and Photonics **9793** (2015) 97930Z. https://doi.org/10.1117/12.2223094
11 W. W. Moses, M. J. Weber, S. E. Derenzo, D. Perry, P. Berdahl, and L. A. Boatner: IEEE Trans. Nucl. Sci. **45** (1998) 462. https://doi.org/10.1109/23.682427
12 L. Ding, Q. Wu, Q. Wang, Y. Li, R. M. Perks, and L. Zhao: EJNMMI Phys. **7** (2020) 60. https://doi.org/10.1186/s40658-020-00327-6
13 E. Takada, Y. Hosono, T. Kakuta, M. Yamazaki, H. Takahashi, and M. Nakazawa: IEEE Trans. Nucl. Sci. **45** (1998) 556. https://doi.org/10.1109/23.682447
14 S. Kodama, S. Kurosawa, M. Ohno, Y. Morishita, H. Usami, M. Hayashi, M. Sasano, T. Azuma, H. Tanaka, V. Kochurikhin, A. Yamaji, M. Yoshino, S. Toyoda, H. Sato, Y. Ohashi, K. Kamada, Y. Yokota, A. Yoshikawa, and T. Torii: Appl. Phys. Express **13** (2020) 047002. https://doi.org/10.35848/1882-0786/ab77f7
15 M. Irshad Ahamed and K. Sathish Kumar: Mater. Sci.-Pol. **37** (2019) 225. https://doi.org/10.2478/msp-2019-0022
16 J. Zhang, Y. Xiang, C. Wang, Y. Chen, S. C. Tjin, and L. Wei: Sensors **22** (2022) 1126. https://doi.org/10.3390/s22031126

17 Z. Yan, G. Gundiah, G. A. Bizarri, E. C. Samulon, S. E. Derenzo, and E. D. Bourret-Courchesne: Nucl. Instrum. Methods Phys. Res. A **735** (2014) 83. https://doi.org/10.1016/j.nima.2013.09.021
18 S. Otake, H. Sakaguchi, Y. Yoshikawa, T. Kato, D. Nakauchi, N. Kawaguchi, and T. Yanagida: Radiat. Meas. **169** (2023) 107032. https://doi.org/10.1016/j.radmeas.2023.107032
19 Q. Liu, P. Ran, W. Chen, N. Shi, W. Zhang, X. Qiao, T. Jiang, Y. M. Yang, J. Ren, Z. Wang, G. Qian, and X. Fan: Ad. Sci. **10** (2023) 2304889. https://doi.org/10.1002/advs.202304889
20 R. Hawrami, E. Ariesanti, A. Farsoni, D. Szydel, and H. Sabet: Crystals **12** (2022) 1517. https://doi.org/10.3390/cryst12111517
21 K. Okazaki, D. Nakauchi, H. Fukushima, T. Kato, N. Kawaguchi, and T. Yanagida: Sens. Mater. **35** (2023) 459. https://doi.org/10.18494/SAM4144
22 M. İlhan, İ. Ç. Keskin, Z. Çatalgöl, and R. Samur: Int. J. Appl. Ceram. Technol. **15** (2018) 1594. https://doi.org/10.1111/ijac.13025
23 S. Otake, H. Sakaguchi, Y. Yoshikawa, T. Kato, D. Nakauchi, N. Kawaguchi, and T. Yanagida: Opt. Mater. **154** (2024) 115747. https://doi.org/10.1016/j.optmat.2024.115747
24 T. Yanagida, K. Kamada, Y. Fujimoto, H. Yagi, and T. Yanagitani: Opt. Mater. **35** (2013) 2480. https://doi.org/10.1016/j.optmat.2013.07.002
25 T. Yanagida, Y. Fujimoto, T. Ito, K. Uchiyama, and K. Mori: Appl. Phys. Express **7** (2014) 062401. https://doi.org/10.7567/APEX.7.062401
26 M. Akatsuka, H. Kimura, D. Onoda, D. Shiratori, D. Nakauchi, T. Kato, N. Kawaguchi, and T. Yanagida: Sens. Mater. **33** (2021) 2243. https://doi.org/10.18494/SAM.2021.3319
27 C. Pfau, C. Bohley, P.-T. Miclea, and S. Schweizer: J. Appl. Phys. **109** (2011) 083545. https://doi.org/10.1063/1.3580281
28 K. Okazaki, D. Nakauchi, T. Kato, N. Kawaguchi, and T. Yanagida: Nucl. Instrum. Methods Phys. Res. B **547** (2024) 165197. https://doi.org/10.1016/j.nimb.2023.165197
29 B. Ahrens, P. T. Miclea, and S. Schweizer: J. Phys.: Condens. Matter **21** (2009) 125501. https://doi.org/10.1088/0953-8984/21/12/125501
30 K. Okazaki, D. Nakauchi, H. Fukushima, T. Kato, N. Kawaguchi, and T. Yanagida: Appl. Sci. **12** (2022) 11624. https://doi.org/10.3390/app122211624
31 S. Takase, K. Miyazaki, D. Nakauchi, T. Kato, N. Kawaguchi, and T. Yanagida: J. Lumin. **267** (2024) 120400. https://doi.org/10.1016/j.jlumin.2023.120400
32 K. Onodera, M. Koshimizu, and K. Asai: Radiat. Phys. Chem. **78** (2009) 1031. https://doi.org/10.1016/j.radphyschem.2009.06.024
33 A. Lu, X. Hu, Y. Lei, Z. Luo, and X. Li: Ceram. Int. **40** (2014) 11. https://doi.org/10.1016/j.ceramint.2013.04.049
34 D. J. Robbins: J. Electrochem. Soc. **127** (1980) 2694. https://doi.org/10.1149/1.2129574